Hindawi
Geofluids
Volume 2021, Article ID 7055693, 11 pages
https://doi.org/10.1155/2021/7055693

Research Article

Deformation Prediction of Foundation Pit Based on Exponential Power Product Model of Improved Algorithm

Chuankui Jing, Hao Wang, and Hongsong Li

CCTEB Infrastructure Construction Investment Co., Ltd., Wuhan 430000, China

Correspondence should be addressed to Chuankui Jing; 18389245349@163.com

Received 2 July 2021; Accepted 25 August 2021; Published 22 October 2021

Academic Editor: Xudong Zhang

In order to improve the prediction accuracy of foundation pit deformation, an improved optimization algorithm of supply and demand-exponential power product foundation pit deformation prediction model (ISDO-EPP model) is proposed. Through six standard test functions and three application examples, the optimization ability of the ISDO algorithm is verified, and the optimization results are compared with those of basic supply demand optimization algorithm (SDO), whale optimization algorithm (WOA), grey wolf optimization algorithm (GWO), moth swarm algorithm (MSA), and particle swarm optimization algorithm (PSO). Taking the settlement prediction of three foundation pits as an example, the delay time and embedding dimension of each case are determined by autocorrelation function method and false nearest neighbor method, and input and output vectors are constructed to train and predict each model. The results show that the search ability of the ISDO algorithm is better than that of SDO and other five algorithms, and the ISDO algorithm has better search accuracy, global search ability, and robustness. The absolute values of average relative errors of the ISDO-EPP model for three cases are 0.73%, 3.36%, and 1.33%, respectively, which are better than ISDO-SVM and ISDO-BP models. It shows that the ISDO algorithm can effectively optimize the parameters of the EPP model, and the ISDO-EPP model is feasible and effective for deformation prediction.

1. Introduction

Effectively improving the prediction accuracy of foundation pit deformation is of great significance for judging the stability of foundation pit, predicting the damage degree of surrounding buildings, and scientifically grasping the future deformation trend of foundation pit. At present, the methods used in deformation prediction include grey prediction method [1, 2], regression method [3, 4], extreme learning machine method [5, 6], support vector machine method [7, 8], artificial neural network method [9–11], and combination prediction method [12, 13], all of which have achieved certain prediction effect in the application of foundation pit deformation prediction, but there are also some shortcomings: the grey prediction method has a high degree of dependence on the original data, and the short-term prediction effect is poor. The regression method is sensitive to outliers and easy to over fit. The application of extreme learning machine is limited by the random determination or artificial customization of connection weights and thresholds between hidden layer nodes. Support vector machine is difficult to select parameters such as penalty factor and kernel function [12]. BP, Elman, and other artificial neural networks are difficult to select the key parameters such as existence weight and threshold and are restricted by the number of samples. The combination forecasting model is too complex, and the weight of each model is difficult to determine. Exponential power product (EPP) is a forecasting model based on the exponential power product relationship between forecasting factors and some influence factors. It has good fitting and forecasting effect for high-dimensional and nonlinear systems, but its disadvantage lies in the reasonable selection of index parameters of influence factors. At present, the EPP model is seldom used in regression prediction.

Choi et al. [14] established the uncertainty model of underground space risk assessment based on fuzzy theory. Kepaptsoglou et al. [15] used analytic hierarchy process (AHP) to evaluate the construction safety risk of Athens metro station. Huang and Bian [16] determined the risk level of deep foundation pit from two aspects: the probability

of occurrence of risk events and the loss consequences. Based on fuzzy membership function and expert scoring method, Lan et al. [17] determined the risk level of deep foundation pit construction. Chen and Guo [18] put forward the method of grey AHP to evaluate the construction safety of subway station. Zhao et al. [19] combined rough set and prior knowledge and determined the weight of safety evaluation index for deep foundation pit construction of subway station. Guo et al. [20] used the expert investigation method to determine the evaluation index affecting the safety of subway deep foundation pit construction and used fuzzy mathematics to determine the safety level. Kang and Wang [21] used data envelopment analysis (DEA) to solve the problem of subjectivity in index weight solving process.

Through the analysis of a large number of foundation pit monitoring data, some scholars summarized and put forward the deformation law and treatment model of foundation pit deformation. In reference [22], the law of deformation of foundation pit and excavation depth in the process of foundation pit construction is studied. In reference [23], the constitutive model was used to study the influence of foundation pit excavation stability. In references [24, 25], based on the analysis of the horizontal displacement and axial force deformation of the support in the foundation pit monitoring of a subway station and Forest Park Station in Beijing, the specific form of the foundation pit supporting structure and the foundation pit deformation monitoring scheme of a subway station in Beijing are proposed, and the deformation law of the maintenance structure in the process of foundation pit excavation is preliminarily obtained. In references [26, 27], the foundation pit of a station in Zhengzhou was monitored during construction, and the monitoring data were processed. According to the local geological conditions, the layout law of monitoring points was analyzed, and the deformation law of foundation pit was studied. In reference [28], the foundation pit construction of a subway station in Nanjing was monitored, and the monitoring results of horizontal displacement of supporting structure, horizontal displacement of pile (wall), ground settlement, pipeline settlement, and support axial force were analyzed. Reference [29] analyzes the important role of pile (wall) horizontal displacement monitoring in foundation pit construction safety and designs the monitoring standard and frequency of pile (wall) horizontal displacement. On the basis of a large number of case studies of deep foundation pit monitoring and through the comparative analysis of different foundation pits, the main factors of deformation of buildings around the foundation pit are summarized in reference [30].

In order to further improve the accuracy of foundation pit deformation prediction and expand the foundation pit deformation prediction model and method, based on the exponential power product relationship between foundation pit deformation prediction factors and influence factors [12], an improved supply-demand-based optimization algorithm EPP foundation pit deformation prediction model (ISDO-EPP model) is proposed, In order to verify the feasibility and effectiveness of the ISDO-EPP model in foundation pit deformation prediction, three examples of foundation pit deformation prediction in references [31–33] are used to test the model.

2. ISDO-EPP Model

2.1. Improved Supply and Demand Optimization Algorithm. Supply and demand optimization (SDO) algorithm is a new metaheuristic optimization algorithm proposed by Zhao et al. [34] in 2019 inspired by economic supply and demand mechanism. The algorithm simulates the demand relationship of consumers and the supply relationship of producers mathematically. By introducing the stable mode and unstable mode of supply and demand mechanism into the SDO algorithm, the two modes are used to perform local search and global search in a given space to solve the problem to be optimized. Compared with the traditional swarm intelligence algorithm, the SDO algorithm has the advantages of fast convergence speed, high optimization accuracy, less adjustment parameters, and better exploration and development ability.

The mathematical description of the SDO algorithm is as follows:

(a)*SDO Algorithm Initialization*. Suppose there are n markets, each market has d different commodities, and each commodity has a certain quantity and price. The price of d commodities in the market represents a group of candidate solutions of the d-dimensional variables of the optimization problem. At the same time, the quantity of d commodities in the market is evaluated as a group of feasible solutions. If the feasible solution is better than the candidate solution, the feasible solution replaces the candidate solution. The price and quantity of commodities in n markets are represented by two matrices: X and Y, respectively.

$$\begin{cases} X = \begin{bmatrix} x_1 \\ x_2 \\ \vdots \\ x_3 \end{bmatrix} = \begin{bmatrix} x_{11} & x_{12} & \cdots & x_{1d} \\ x_{21} & x_{22} & \cdots & x_{2d} \\ \vdots & \vdots & \ddots & \vdots \\ x_{n1} & x_{n2} & \cdots & x_{nd} \end{bmatrix}, \\ Y = \begin{bmatrix} y_1 \\ y_2 \\ \vdots \\ y_3 \end{bmatrix} = \begin{bmatrix} y_{11} & y_{12} & \cdots & y_{1d} \\ y_{21} & y_{22} & \cdots & y_{2d} \\ \vdots & \vdots & \ddots & \vdots \\ y_{n1} & y_{n2} & \cdots & y_{nd} \end{bmatrix}, \end{cases} \tag{1}$$

where x_i and y_i are the price and quantity of the i commodity, respectively, and x_{ij} and y_{ij} are the price and quantity of the j commodity in the i market, respectively.

The fitness function is used to evaluate the price and quantity of goods in each market, for n markets, the fitness of commodity price and quantity are as follows:

$$\begin{cases} F_x = (F_{x1}, F_{x2}, \cdots, F_{xn}), \\ F_y = (F_{y1}, F_{y2}, \cdots, F_{yn}). \end{cases} \tag{2}$$

(b)*Equilibrium Quantity and Equilibrium Price.*

Assuming that the equilibrium price x_0 and equilibrium quantity y_0 of each commodity are variable in each iteration process, a commodity quantity is selected from the commodity quantity set of each market as its quantity equilibrium vector. The larger the market fitness value is, the greater the probability of the selected commodity quantity in each market is. At the same time, each market can also choose a commodity price from the commodity price set according to its probability or take the average value of all market commodity prices as the equilibrium price. The equilibrium quantity of goods y_0 is expressed as follows:

$$\begin{aligned} y_0 &= y_k\, k = R(Q), \\ Q &= \frac{F_y}{\sum_{i=1}^{n} F_{yi}} \left| F_{yi} - \frac{1}{n}\sum_{i=1}^{n} F_{yi} \right|, \end{aligned} \tag{3}$$

where $F_{yi} = \begin{cases} 1/1 + f(y_i) & f(y_i) > 0 \\ 1/1 - f(y_i) & f(y_i) \le 0 \end{cases}$,where $f(y_i)$ is the fitness value of commodity quantity y_i and $R(.)$ is roulette wheel selection.

The commodity equilibrium price x_0 is expressed as follows:

$$\begin{aligned} x_0 &= \begin{cases} r\dfrac{\sum_{i=1}^{n} x_i}{n} & r_1 < 0.5, \\ x_k,\, k = R(P) & r_1 \ge 0.5, \end{cases} \\ P &= \frac{F_x}{\sum_{i=1}^{n} F_{xi}} \left| F_{xi} - \frac{1}{n}\sum_{i=1}^{n} F_{xi} \right|, \end{aligned} \tag{4}$$

where $F_{xi} = \begin{cases} 1/1 + f(x_i) & f(x_i) > 0 \\ 1/1 - f(x_i) & f(x_i) \le 0 \end{cases}$,where $f(x_i)$ is the fitness value of commodity price x_i and r and r_1 are the random numbers in [0,1].

(c)*Supply Function and Demand Function*. According to equilibrium quantity y_0 and equilibrium price x_0, supply function and demand function are given, respectively:

$$y_{i,t+1} = y_0 - \alpha(x_{i,t} - x_0), \tag{5}$$

$$x_{i,t+1} = x_0 + \beta(y_{i,t+1} - y_0), \tag{6}$$

where $x_{i,t}$ and $y_{i,t}$ are the price and quantity of the i commodity in the t iteration, respectively, and α and β are demand weight and supply weight, respectively. Update the equilibrium price and equilibrium quantity by adjusting α and β.

If Equation (5) is inserted into Equation (6), the demand formula can be rewritten as follows:

$$x_{i,t+1} = x_0 - \alpha\beta(x_{i,t} - x_0), \tag{7}$$

The supply weight α and demand weight β are as follows:

$$\alpha = \frac{2(T - t + 1)}{T} \sin(2\pi r), \tag{8}$$

$$\beta = 2\cos(2\pi r), \tag{9}$$

where T is the maximum number of iterations. The variable L is produced by the weight supply α and the demand weight β. We can get the following results:

$$L = \alpha\beta = \frac{4(T - t + 1)}{T} \sin(2\pi r)\cos(2\pi r). \tag{10}$$

The variable L is helpful to the smooth transition of the SDO algorithm between exploration and development. $|L| < 1$ is a stable mode, and by adjusting the supply weight α and demand weight β, different commodity prices around the equilibrium price x_0 are obtained. These commodity prices can change randomly between the current price and the equilibrium price through the random number r. The stable mode mechanism emphasizes "development" to improve the local exploration ability of the SDO algorithm. $|L| < 1$ is an unstable mode, which allows the commodity price in any market to be far away from the equilibrium price. The mechanism of unstable mode forces each market to "explore" the unknown area in the search space to improve the global search ability of the SDO algorithm.

In order to speed up the convergence speed of the SDO algorithm and further improve the local exploration performance and global search ability of SDO, the weights are supplied α. The improved operator is as follows:

$$\alpha = 2\left(\frac{T - t + 1}{T}\right)^{10(1 - t/T)} \sin(2\pi r). \tag{11}$$

2.2. Exponential Power Product Model. The results show that there is an exponential power product (EPP) relationship between the prediction factors and the influence factors of foundation pit deformation as shown in Equation (12) [35]:

$$y' = \prod_{j=1}^{m} \left(x_1'\right)^{a_1} \left(x_2'\right)^{a_2} \cdots \left(x_m'\right)^{a_m}, \tag{12}$$

where y' is the normalized value of foundation pit deformation prediction factor, x_j' is the normalized value of influence factor related to the prediction factor of foundation pit deformation, a_j is the index parameter to be optimized, and m is the number of predictive impact factors.

2.3. Implementation Steps of ISDO-EPP Model Prediction. The implementation steps of ISDO-EPP model prediction are summarized as follows:

Step 1. Determine the delay time and embedding dimension of the foundation pit settlement data by AFM and FNN, construct the input and output vectors of the EPP model, reasonably divide the training samples and prediction

samples, and normalize the case data series by formula (13). Set the search range of the EPP model index parameters a_j.

$$x' = \frac{(x - 0.8x_{\min})}{(1.2x_{\max} - 0.8x_{\min})}, \tag{13}$$

where x' is the normalized data, x is the original data, and $x_{\max}$ and $x_{\min}$ are the maximum and minimum values in the sequence, respectively.

Step 2. Determine the optimization objective function. The mean square error is selected as the optimization objective function:

$$\begin{cases} \min f(a_1, a_2, \cdots, a_m) = \dfrac{1}{M}\sum_{i=1}^{M}(y_i - y\wedge_i)^2, \\ s.t \qquad\qquad a \in [a_{\min}, a_{\max}], \end{cases} \tag{14}$$

where $\widehat{y_i}$ is the prediction output of the i sample, y_i is the monitoring value of the i sample, and M is the number of training samples.

Step 3. Set the number of SDO market groups N, the maximum number of iterations T, the problem dimension, and the search space. Initialize the commodity price x_i and quantity y_i randomly, so that the current iteration number $T = 0$.

Step 4. Calculate the fitness values F_{xi} and F_{yi} of commodity price x_i and commodity quantity y_i based on Equation (14). If F_{yi} is better than F_{xi}, y_i is used instead of x_i and save x_{best} as the current optimal solution.

Step 5. Use Equation (11) and Equation (13) to determine the supply weight α and demand weight β.

Step 6. For each market, use Equation (3) to determine the equilibrium quantity y_0. Use Equation (4) to determine the equilibrium price x_0.

Step 7. Update the quantity of goods y_i by formula (5). Use formula (6) to update commodity price x_i. The fitness values F_{xi} and F_{yi} of commodity price x_i and commodity quantity y_i are calculated based on formula (14). If F_{yi} is better than F_{xi}, y_i is used instead of x_i, and x_{best} is saved as the current optimal solution.

Step 8. Where $t = t + 1$, judge whether the algorithm reaches the termination condition, and if so, output the optimal solution x_{best}, and the algorithm ends. Otherwise, repeat Steps 5–8.

Step 9. Output the SDO algorithm global optimal solution x_{best}, and x_{best} is the best index parameter a_j of the EPP model. The index parameter a_j is substituted into the EPP model to predict the deformation of foundation pit.

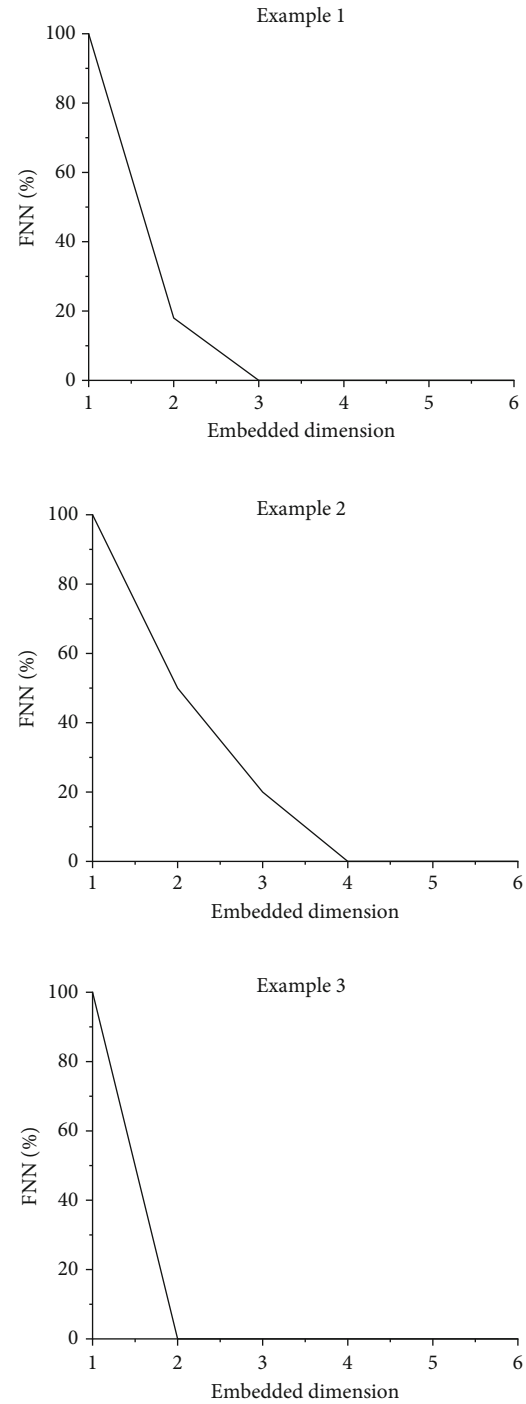

Figure 1: Results of false neighbor method for foundation pit monitoring data.

3. Example Application

3.1. Data Sources and Analysis. In this paper, three examples of foundation pit deformation prediction in reference [14–16] are used for verification. Firstly, AFM is used to determine the delay time of settlement data. After analysis, when the delay time is 1, the autocorrelation coefficients of the three cases are the largest, which are 0.938, 0.779, and 0.786, respectively. Therefore, the delay time of settlement

Table 1: Comparison results of function optimization.

Function	Algorithm	Average value		Standard deviation	
		30 dimensions	5 dimensions	30 dimensions	5 dimensions
Sphere	ISDO	$4.03 * 10^{-118}$	$7.40 * 10^{-125}$	$8.55 * 10^{-118}$	$1.33 * 10^{-124}$
	SDO	$8.42 * 10^{-50}$	$2.22 * 10^{-61}$	$1.98 * 10^{-49}$	$4.40 * 10^{-61}$
	WOA	$3.38 * 10^{-32}$	$2.67 * 10^{-37}$	$7.20 * 10^{-30}$	$5.71 * 10^{-37}$
	GWO	$6.01 * 10 * ^{11}$	$3.34 * 10^{-45}$	$7.47 * 10^{-11}$	$7.38 * 10^{-45}$
	MSA	$5.16 * 10^{-72}$	$1.68 * 10^{-86}$	$1.25 * 10^{-71}$	$6.59 * 10^{-86}$
	PSO	$8.29 * 10^{2}$	$4.01 * 10^{-4}$	$2.46 * 10^{2}$	$7.56 * 10^{-4}$
Schwefel 2.22	ISDO	$5.36 * 10^{-62}$	$7.99 * 10^{-65}$	$8.19 * 10^{-62}$	$1.02 * 10^{-64}$
	SDO	$1.04 * 10^{-27}$	$9.19 * 10^{-33}$	$1.34 * 10^{-27}$	$1.05 * 10^{-32}$
	WOA	$3.57 * 10^{-2}$	$3.19 * 10^{-24}$	$4.55 * 10^{-21}$	$5.51 * 10^{-24}$
	GWO	$3.70 * 10^{-7}$	$7.67 * 10^{-26}$	$1.71 * 10^{-7}$	$1.62 * 10^{-25}$
	MSA	$1.41 * 10^{-38}$	$5.31 * 10^{-44}$	$2.58 * 10^{-38}$	$7.37 * 10^{-44}$
	PSO	36.6	$2.87 * 10^{-4}$	24.7	$1.43 * 10^{-4}$
Schwefel 2.21	ISDO	$1.46 * 10^{-111}$	$3.27 * 10^{-120}$	$3.55 * 10^{-111}$	$7.83 * 10^{-120}$
	SDO	$1.26 * 10^{-38}$	$5.16 * 10^{-51}$	$2.71 * 10^{-38}$	$1.11 * 10^{-50}$
	WOA	$6.33 * 10^{4}$	61.8	$1.38 * 10^{4}$	86.7
	GWO	36.7	$4.12 * 10^{-24}$	45.7	$9.54 * 10^{-24}$
	MSA	$5.03 * 10^{-52}$	$1.78 * 10^{-69}$	$1.22 * 10^{-51}$	$3.81 * 10^{-69}$
	PSO	$1.43 * 10^{4}$	56.2	$8.09 * 10^{3}$	76.1
Griewank	ISDO	0	0	0	0
	SDO	0	$7.61 * 10^{-14}$	0	$1.83 * 10^{-14}$
	WOA	$1.51 * 10^{-17}$	10.3	$3.56 * 10^{-17}$	13.4
	GWO	$7.59 * 10^{-3}$	$5.97 * 10^{-2}$	$1.08 * 10^{-2}$	$6.32 * 10^{-2}$
	MSA	0	0	0	0
	PSO	$4.52 * 10^{2}$	$2.83 * 10^{1}$	$3.29 * 10^{1}$	$1.18 * 10^{1}$
Rastrigin	ISDO	0	0	0	0
	SDO	0	0	0	0
	WOA	$5.16 * 10^{-15}$	3.66	$1.26 * 10^{-14}$	6.51
	GWO	1.23	$8.55 * 10^{-44}$	4.59	$1.80 * 10^{-43}$
	MSA	0	0	0	0
	PSO	42.3	2.62	9.42	1.24
Ackley	ISDO	8.88 * 10 – 16	8.88 * 10 – 16	1.97 * 10 – 31	1.97 * 10 – 31
	SDO	8.88 * 10 – 16	8.88 * 10 – 16	1.97 * 10 – 31	1.97 * 10 – 31
	WOA	9.93 * 10 – 15	7.83 * 10 – 15	3.81 * 10 – 15	4.82 * 10 – 15
	GWO	1.35 * 10 – 6	5.41 * 10 – 15	6.21 * 10 – 7	1.54 * 10 – 15
	MSA	3.15 * 10 – 15	2.82 * 10 – 15	1.69 * 10 – 15	1.77 * 10 – 15
	PSO	2.01	4.09 * 10 – 4	1.25	2.81 * 10 – 4

data is 1. Secondly, when the delay time is 1, FNN is used to determine the embedding dimension of settlement data, as shown in Figure 1. It can be seen from Figure 1 that when the embedding dimensions are 3, 4, and 2, the proportion of false nearest neighbors of the three instances is 0, which is less than 1%, indicating that the reconstructed attractor determined by the embedding dimension will no longer overlap due to projection into the low dimensional space, that is, when the delay time is 1 and the embedding dimensions are 3, 4, and 2, the three instances have the best prediction effect. Finally, when the delay time is 1 and the embedding dimension is 3, 4, and 2, respectively,

Table 2: Comparison results of objective function optimization of application examples.

	Algorithm	$T = 200$		$T = 500$	
		Average value	Standard deviation	Average value	Standard deviation
Example 1	ISDO	4.3678	$7.99 * 10^{-8}$	4.3678	$8.88 * 10^{-16}$
	SDO	4.3679	$2.18 * 10^{-5}$	4.3678	$3.02 * 10^{-8}$
	WOA	90.0952	75.4986	36.4155	45.4613
	GWO	4.8315	42.2	4.6506	31.3
	MSA	7.3969	3.1339	5.3188	1.2160
	PSO	4.3733	$8.23 * 10^{-5}$	4.3679	$1.75 * 10^{-4}$
Example 2	ISDO	2.0595	$2.93 * 10^{-8}$	2.0595	$1.33 * 10^{-15}$
	SDO	2.0595	$2.85 * 10^{-5}$	2.0595	$7.74 * 10 * 8$
	WOA	45.6086	40.2625	30.6689	24.5341
	GWO	6.4553	3.6920	5.4012	2.2957
	MSA	7.1709	2.3879	5.1287	1.1907
	PSO	2.0762	$1.58 * 10^{-2}$	2.0603	$9.83 * 10^{-4}$
Example 3	ISDO	2.0020	0	2.0020	0
	SDO	2.0020	0	2.0020	0
	WOA	14.4174	16.8726	2.7690	1.1773
	GWO	2.0557	13.1	2.0020	$2.13 * 10^{-6}$
	MSA	2.0032	$1.99 * 10^{-3}$	2.0020	$3.72 * 10^{-6}$
	PSO	2.0020	$5.80 * 10^{-7}$	2.0020	0

the foundation pit settlement values of the first three periods of case 1, the first four periods of case 2, and the first two periods of case 3 are predicted by using the monitoring data of the first three periods of case 1, the fifth period of case 2, and the third period of case 3, and the measured data of the first 32 periods and the first 11 periods of case 1, case 2, and case 3 are selected as the training samples, and the last five periods are selected as the prediction samples. In case 3, the first 10 periods of measured data are selected as training samples, and the last three periods of data are selected as prediction samples. Limited to space, the input and output matrix of foundation pit deformation prediction factor and influence factor is omitted.

3.2. Algorithm Verification

3.2.1. Simulation Verification of Standard Test Function. In order to verify the optimization ability of the ISDO algorithm in high-dimensional (30 dimensions) and low dimensional (5 dimensions) conditions, the ISDO algorithm is used to simulate Sphere, Schwefel 2.22, Schwefel 2.21, Griewank, Rastrigin, and Ackley 6 typical test functions, and the simulation results are compared with SDO, WOA, GWO, MSA, and PSO algorithms. The value ranges of the above 6 function variables are, respectively [-100, 100], [-10, 10], [-100, 100], [-600, 600], [-5.12, 5.12], and [-32, 32], with dimensions of 30 and 5, and the theoretical optimal solution values are all 0. Among them, Sphere, Schwefel 2.22, and Schwefel 2.21 are unimodal functions, which are mainly used to test the optimization accuracy of the algorithm. The functions Griewank, Rastrigin, and Ackley are multimodal functions, which are mainly used to test the global search ability of the algorithm. Based on MATLAB 2018a M language, 6 algorithms are implemented to optimize 6 typical test functions 20 times and evaluated from two aspects of average value and standard deviation, as shown in Table 1. The experimental parameters are set as follows: the maximum number of iterations of the six algorithms is $T = 200$, and the number of groups is $N = 50$. The shape constant of WOA logarithmic helix $b = 2$. The number of exploration moths MSA n_p=5. The inertia weight of the PSO algorithm $w_{\max}$ and $w_{\min}$ are 0.9 and 0.6, respectively, and the self-learning factor c_1 and social learning factor c_2 are 2.0. Other parameters adopt the default values of each algorithm.

(a) For Sphere and Schwefel 2.22 of unimodal function, the ISDO algorithm is slightly better than MSA, SDO, WOA, and GWO algorithms and far better than the PSO algorithm in high and low dimensions. For the gradient function Schwefel 2.21, the ISDO algorithm is superior to MSA and SDO algorithms in 20 times of optimization accuracy in high dimension and is far superior to WOA, GWO, and PSO algorithms. Under the condition of low dimension, the ISDO algorithm is slightly better than MSA and SDO algorithms, better than the GWO algorithm, and far better than WOA and PSO algorithms. For unimodal functions, the ISDO algorithm shows good optimization accuracy in both high and low dimensional conditions

Table 3: Comparison of deformation prediction models of each foundation pit.

Example	Model	Periods	Measured value/mm	Estimate/mm	Absolute error/%	Relative error/%	MRE/%	MAE/mm
		36	22.24	22.27	-0.1	-0.45		
		37	22.96	23.19	0.23	1		
	ISDO-EPP	38	23.75	23.68	-0.07	-0.29	0.73	0.17
		39	24.45	24.57	0.12	0.47		
		40	24.84	25.19	0.35	1.42		
		36	22.24	22.12	-0.22	-0.97		
		37	22.96	23.02	0.06	0.26		
1	ISDO-SVM	38	23.75	23.65	-0.1	-0.43	0.81	0.19
		39	24.45	24.57	0.12	0.48		
		40	24.84	25.32	0.48	1.92		
		36	22.24	22.26	-0.08	-0.34		
		37	22.96	23.25	0.25	1.25		
	ISDO-BP	38	23.75	23.74	-0.01	-0.04	0.87	0.21
		39	24.45	24.66	0.21	0.87		
		40	24.84	25.29	0.45	1.83		
		16	11.3	11.14	-0.16	-1.44		
		17	12.1	11.76	-0.34	-2.79		
	ISDO-EPP	18	12.3	12.72	0.42	3.42	3.36	0.43
		19	13.5	12.48	-1.02	-7.55		
		20	14.7	14.47	-0.23	-1.59		
		16	11.3	11.49	0.19	1.67		
		17	12.1	11.75	-0.35	-2.82		
2	ISDO-SVM	18	12.3	12.52	0.22	1.81	3.83	0.51
		19	13.5	12.72	-0.78	-5.81		
		20	14.7	13.68	-1.02	-6.92		
		16	11.3	11.19	-0.11	-1.01		
		17	12.1	11.39	-0.71	-5.86		
	ISDO-BP	18	12.3	12.11	-0.19	-1.58	5.96	0.81
		19	13.5	12.17	-1.33	-9.87		
		20	14.7	13.01	-1.69	-11.48		
		13	13.86	13.81	-0.05	-0.35		
	ISDO-EPP	14	15.12	15.19	0.07	0.49	1.33	0.22
		15	16.84	16.31	-0.53	-3.14		
		13	13.86	13.04	-0.82	-5.9		
3	ISDO-SVM	14	15.12	14.46	-0.66	-4.36	5.83	0.90
		15	16.84	15.62	-1.22	24		
		13	13.86	12.79	-1.07	-7.75		
	ISDO-BP	14	15.12	14.12	-1	-6.61	8.01	1.23
		15	16.84	15.21	-1.63	-9.66		

(b) For the multimodal function Griewank, ISDO and MSA all obtain the theoretical optimal value of 0 in the case of high dimension and low dimension. The optimization accuracy is better than the SDO algorithm and far better than WOA, GWO, and PSO algorithms. For the multimodal function Rastrigin which is easy to fall into local extremum, ISDO, SDO, and MSA all obtain the theoretical optimal value 0 in high and low dimensions, and the optimization accuracy is much better than WOA, GWO, and PSO. For continuous rotation nonseparable multimodal function Ackley, ISDO algorithm and SDO algorithm all obtain the relative theoretical optimal value $8.88 * 10^{-16}$ after 20 times of optimization, and the optimization accuracy is better than MSA, WOA, and GWO algorithms and far better than the PSO algorithm. For multimodal functions, the ISDO algorithm has better global search ability in both high and low dimensions

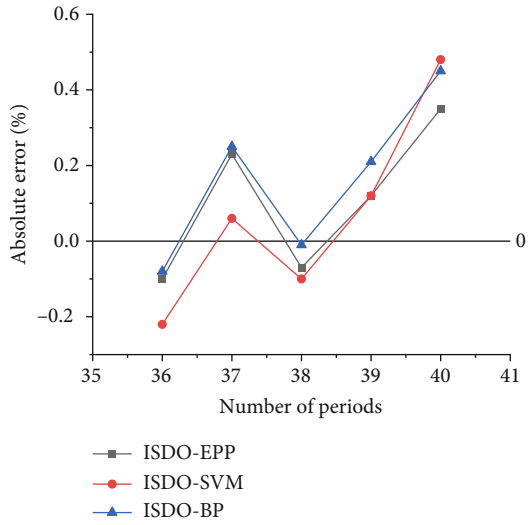

Figure 2: Absolute error of three models in example 1.

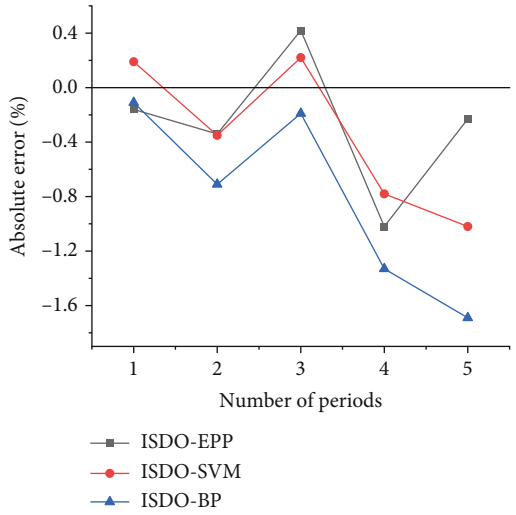

Figure 3: Absolute error of three models in example 2.

(c) From the simulation results of 6 standard test functions, the optimization accuracy of ISDO, MSA, and SDO algorithms is not affected by dimension. For the more difficult to optimize Schwefel 2.21, Griewank, and Rasrigin functions, the optimization accuracy of WOA, GWO, and PSO algorithms is greatly affected by dimension changes. In a word, the 6 algorithms have the following order: ISDO, MSA, SDO, GWO, WOA, and PSO

3.2.2. Example Objective Function Optimization Verification. In order to verify the optimization performance of ISDO, SDO, WOA, GWO, MSA, and PSO algorithms in practical application, the optimization performance of ISDO and other 6 algorithms is verified by using the three optimization objective functions constructed above, namely, Equation (14). Among them, the search range of the EPP model parameters is [-5,5], the maximum number of iterations T is set to 200 and 500, and other parameter settings and evaluation indexes are the same as above. The example optimization results are shown in Table 2.

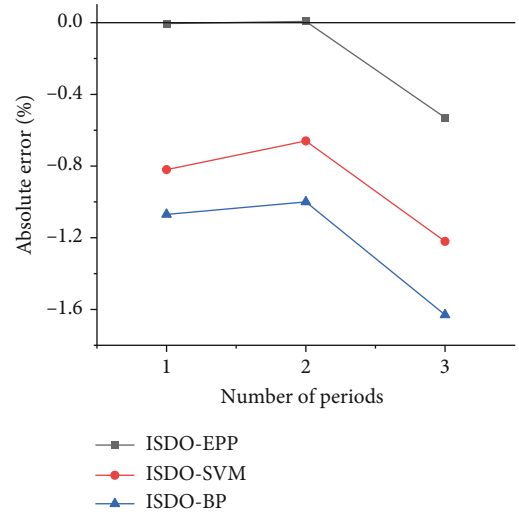

Figure 4: Absolute error of three models in example 3.

For example 1, for the ISDO algorithm, the optimal value of the objective function is 4.3678, and the standard deviation is less than $8.88 * 10^{-8}$, which is better than the SDO algorithm under the same conditions, better than PSO and GWO algorithm, and far better than MSA and WOA. For example 2, the minimum value of the objective function of ISDO and SDO algorithms is 2.0595 under different iteration conditions, which is better than the PSO algorithm and much better than GWO, MSA, and WOA algorithms. For example 3, because the sequence is short and the dimension to be optimized is low, the minimum value of the objective function of ISDO, SDO, and PSO algorithms for 20 times of optimization is 2.0020, and the standard deviation is 0. The optimization effect is better than MSA and GWO algorithms under the same conditions and far better than WOA.

MSA, GWO, and WOA, which have good performance in the above 6 standard test functions, have poor performance in the optimization of the three examples, and the optimization effect is even lower than that of the PSO algorithm, which can be considered as a failure. The "no free lunch theorem" is verified by an example of optimal parameter optimization, that is, no algorithm can solve all optimization problems. In summary, the order of the optimization accuracy of the six algorithms in the application example is ISDO, SDO, PSO, MSA, GWO, and WOA.

It can be seen that the improved ISDO algorithm based on supply weight can further improve the balance ability of the SDO algorithm between exploration and development and improve the convergence speed and global search performance of the SDO algorithm; the ISDO algorithm not only has better convergence accuracy and global search ability under high and low dimensional conditions of standard test function, but also shows good optimization effect and robustness in the case of objective function optimization.

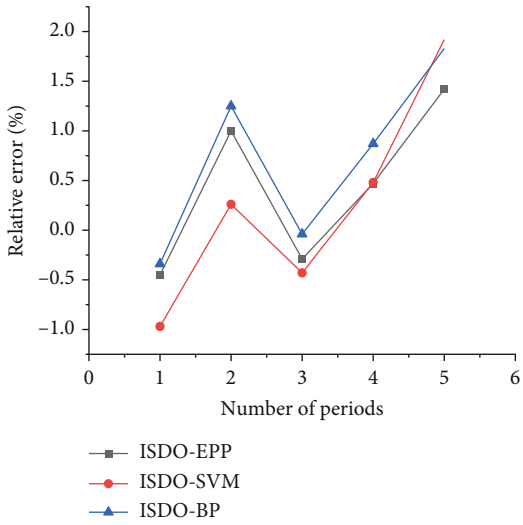

Figure 5: Relative error of three models in example 1.

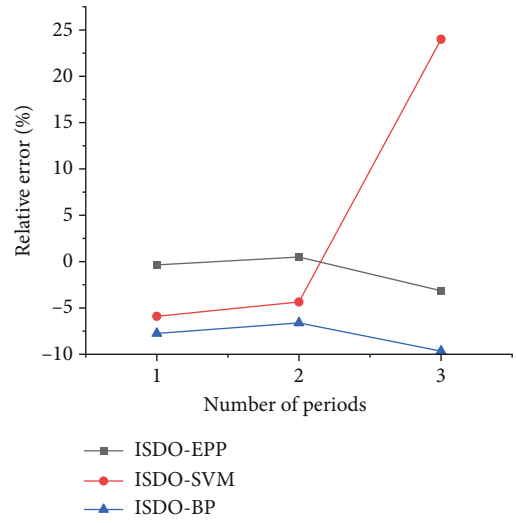

Figure 7: Relative error of three models in example 3.

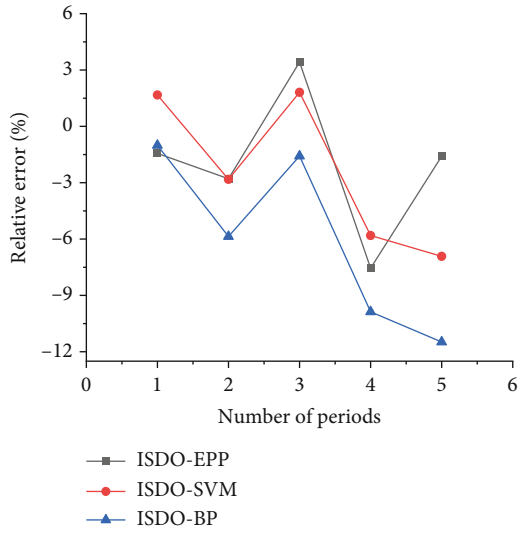

Figure 6: Relative error of three models in example 2.

3.3. Example Prediction and Analysis. ISDO-EPP, ISDO-SVM, and ISDO-BP models are constructed, respectively, to predict the deformation of the foundation pit of the above three examples under the condition that the maximum number of iterations is 200. MRE and MAE are selected as evaluation indexes, and three models are used to predict the foundation pit deformation of three examples. The results are shown in Table 3, and the effect chart of training prediction relative error is given, as shown in Figure 2. The parameters of SVM and BP are set as follows: SVM model penalty factor $C \in [0.1, 1000]$, kernel function parameter $g \in [0.1, 1000]$, insensitive coefficient $\varepsilon \in [0.001, 0.1]$, and the fold number of cross validation $V = 3$. Three examples of BP model network structure were set as 3-5-1, 4-7-1, and 2-3-1, the transfer functions of hidden layer and output layer were logsig and purelin, the training functions were trainlm, the expected error was 0.001, the maximum training cycle was 100 times, and the search space was [-1, 1].

According to Tables 2 and 3 and Figures 2–7, the following conclusions can be drawn:

(a) The MRE of the ISDO-EPP model for three cases is 0.73%, 3.83%, and 1.33%, respectively, and the accuracy is 9.9%, 12.3%, and 77.2% higher than the ISDO-SVM model and 16.1%, 43.6%, and 83.4% higher than the ISDO-BP model. The MAE of the three examples is 0.17 mm, 0.51 mm, and 0.22 mm, respectively. The accuracy is 10.5%, 15.7%, and 75.6% higher than that of the ISDO-SVM model and 19.0%, 46.9%, and 82.1% higher than that of the ISDO-BP model. The results show that the ISDO algorithm can effectively optimize the index parameters of the EPP model, and the ISDO-EPP model is feasible and effective for foundation pit deformation prediction; the model and method can provide a new way and method for dam deformation prediction

(b) From Figure 2 and Tables 2 and 3, the fitting accuracy (optimization result of objective function) and prediction accuracy of the ISDO-EPP model are better than ISDO-SVM and ISDO-BP models, which shows that the ISDO-EPP model has better fitting and prediction accuracy; It can be seen from Table 2 that the results of ISDO algorithm's 20 times of optimization of EPP model's objective function are the same, that is, the results of optimization parameters are the same, which indicates that the ISDO-EPP model has good robustness

(c) According to the comparative analysis of the prediction results of three models on three cases, the ISDO-EPP model has good applicability and prediction effect, and the prediction results are credible and

reasonable. The prediction effect of the ISDO-BP model is not very ideal because there are too few training samples to fully train the model, and it is easy to appear "over fitting" or "under fitting" phenomenon in the process of practical application, resulting in poor practical performance of the model

4. Conclusion

(1) An improved supply and demand optimization (ISDO) algorithm is proposed. The optimization ability of the ISDO algorithm is verified by six typical test functions in high and low dimensions and three example objective functions, and the optimization results are compared with SDO, WOA, GWO, MSA, and PSO algorithms. The results show that the ISDO algorithm not only has better convergence accuracy and global search ability under the high and low dimensional conditions of the standard test function, but also shows good optimization effect and robust performance in the case of objective function optimization

(2) Based on AFM and FNN, the delay time and embedding dimension of settlement data are determined, and the input and output vectors of foundation pit deformation prediction are constructed; the ISDO algorithm is used to optimize the index parameters of the EPP model, and the ISDO-EPP model is proposed. ISDO-SVM and ISDO-BP models are constructed as comparison models. Three examples of foundation pit deformation prediction are compared and verified. The results show that the prediction accuracy and effect of the ISDO-EPP model are better than those of ISDO-SVM and ISDO-BP models, and it has better fitting prediction accuracy and robustness. It shows that the ISDO algorithm can effectively optimize the index parameters of the EPP model, and the ISDO-EPP model is feasible and effective for foundation pit deformation prediction

(3) The verification shows that MSA, GWO, and WOA, which perform better in the standard test function, perform worse in the optimization of three examples, and the optimization effect is even lower than that of the PSO algorithm, so it can be considered that the optimization fails. The "no free lunch theorem" is verified again, that is, no algorithm can solve all optimization problems

Data Availability

The data used to support the findings of this study are included within this article.

Conflicts of Interest

The authors declare that there is no conflict of interest regarding the publication of this paper.

References

[1] X. K. Wang and J. Wang, "Study of deformation prediction of foundation pit based on optimized support vector machine-chaotic BP neural network," *Tunnel Construction*, vol. 37, no. 9, pp. 1105–1113, 2017, (in Chinese).

[2] C. Y. Liu, Y. Wang, X. M. Hu, Y. L. Han, X. P. Zhang, and L. Z. du, "Application of GA-BP neural network optimized by Grey Verhulst model around settlement prediction of foundation pit," *Geofluids*, vol. 2021, 16 pages, 2021.

[3] X. S. Deng, S. Q. Chen, and Z. C. Yin, "Application of dynamic regression model in deformation analysis," *Journal of Geodesy and Geodynamics*, vol. 31, no. 5, pp. 132–135, 2011, (in Chinese).

[4] X. Zhang, E. Zhai, Y. Wu, D. Sun, and Y. Lu, "Theoretical and numerical analyses on hydro–thermal–salt–mechanical interaction of unsaturated salinized soil subjected to typical unidirectional freezing process," *International Journal of Geomechanics*, vol. 21, no. 7, article 04021104, 2021.

[5] Y. Wu, E. Zhai, X. Zhang, G. Wang, and Y. Lu, "A study on frost heave and thaw settlement of soil subjected to cyclic freeze-thaw conditions based on hydro-thermal-mechanical coupling analysis," *Cold Regions Science and Technology*, vol. 188, p. 103296, 2021.

[6] J. Zhu, "Study on deformation law of foundation pit by multifractal detrended fluctuation analysis and extreme learning machine improved by particle swarm optimization," *Journal of Yangtze River Scientific Research Institute*, vol. 36, no. 3, pp. 53–58, 2019, (in Chinese).

[7] T. F. Feng, X. S. Liu, Y. Zhong, and Y. Liang, "Research on deformation prediction based on LSSVR optimized by IABC," *Journal of Geodesy and Geodynamics*, vol. 39, no. 1, pp. 98–102, 2019, (in Chinese).

[8] X. N. Wang and G. F. Han, "Study of application of trend term separation prediction mode and rescaled range (R/S) analysis to deformation prediction of deep foundation pit," *Tunnel Construction*, vol. 37, no. 8, pp. 79–85, 2017, (in Chinese).

[9] Z.-F. Yang, L. Luo, D.-Y. Jia, and X. Tang, "Prediction of deep foundation pit deformation based on wavelet de-noising," *Yangtze River*, vol. 2014, p. 19, 2014.

[10] Z. Jia, Q. J. Guo, and Q. W. Hao, "Deformation prediction of deep foundation pit based on Elman-Markov model," *Yangtze River*, vol. 50, no. 1, pp. 202–206, 2019, (in Chinese).

[11] C. Liu, X. Hu, R. Yao et al., "Assessment of soil thermal conductivity based on BPNN optimized by genetic algorithm," *Advances in Civil Engineering*, vol. 2020, 2020.

[12] F. Wang, "Combined prediction analysis and safety evaluation of foundation pit deformation," *Tunnel Construction*, vol. 39, no. 2, pp. 38–44, 2019, (in Chinese).

[13] B. Jia and L. Wu, "Research of prediction of foundation deformation based on gray BP neural network combined model," *Tunnel Construction*, vol. 29, no. 3, pp. 280–283, 2009, (in Chinese).

[14] H. H. Choi, H. N. Cho, and J. W. Seo, "Risk assessment methodology for underground construction projects," *Journal of Construction Engineering and Management*, vol. 130, no. 2, pp. 258–272, 2004.

[15] K. Kepaptsoglou, M. G. Karlaftis, and J. Gkountis, "A fuzzy AHP model for assessing the condition of metro stations," *KSCE Journal of Civil Engineering*, vol. 17, no. 5, pp. 1109–1116, 2013.

[16] H. W. Huang and Y. H. Bian, "Risk management in the construction of deep excavation engineering," *Chinese Journal of Underground Space and Engineering*, vol. 11, no. 4, pp. 611–614, 2005, 645.

[17] S. Q. Lan and Q. H. Zhang, "Risk assessment of deep excavation during construction based on fuzzy theory," *Chinese Journal of Geotechnical Engineering*, vol. 10, no. 4, pp. 648–652, 2009.

[18] W. K. Chen and M. Y. Guo, "Application of safety evaluation model of subway construction based on gray correlation theory," *Journal of Engineering Management*, vol. 8, no. 5, pp. 52–56, 2014.

[19] J. X. Zhao, M. Liu, F. Li, and K. Fan, "Research on safety management of drilling-blasting metro station construction based on rough set and attribute comprehensive evaluation," *Safety and Environmental Engineering*, vol. 22, no. 5, pp. 113–117, 2015.

[20] J. Guo, J.-D. Qian, J. Chen, J. Yin, and X.-F. Ke, "Risk identification and evaluation for foundation pit construction of subway station," *Journal of Civil Engineering and Management*, vol. 34, no. 5, pp. 32–38, 2017.

[21] L. L. Kang and Q. Wang, "Fire safety evaluation of high-rise building based on dea and gray clustering," *Industrial Safety and Environmental Protection*, vol. 43, no. 7, pp. 29–33, 2017, 37.

[22] M. Long, "Database for retaining wall and ground movements due to deep excavations," *Journal of Geotechnical and Geoenvironmental Engineering*, vol. 127, no. 3, pp. 203–224, 2001.

[23] R. J. Finno, T. J. Blackbum, and J. E. Roboskl, "Three-dimensional effects for supported engineering in clay," *Journal of Geotechnical & Geoenvironmental Engineering*, vol. 133, no. 1, pp. 30–36, 2007.

[24] J.-X. Ren, L.-X. Gao, J. Liu, K. Zhang, and P. Chi, "In-situ monitoring on deformation laws of deep foundation pit," *Journal of Xi'an University of Science and Technology*, vol. 28, no. 3, pp. 445–449, 2008.

[25] J.-X. Ren, X.-G. Feng, H. Liu, and X.-C. Qin, "Research on the deformation law of supporting structure for deep foundation pit of metro station," *Journal of Railway Engineering Society*, vol. 26, no. 3, pp. 89–92, 2009.

[26] J. J. Lan, Y. P. Liu, and J. Song, "Study on deformation of foundation pit based on B Pneural network and Matlab," *Journal of Henan University of Urban Construction*, vol. 26, no. 4, pp. 13–18, 2017.

[27] T.- L. Chen, X.-L. Pan, A.-M. Wang, and Z.-Q. Huang, "Survey and analysis of a foundation pit in Zhengzhou," *Journal of North China Institute of Water Conservancy and Hydroelectric Power*, vol. 29, no. 5, pp. 76–78, 2008.

[28] J. Hu and J. Du, "A discussion of observing method forconcrete-face deformation," *Dam Observation and Geotechnical Tests*, vol. 21, no. 2, pp. 31–37, 1997.

[29] C. B. He, "Obliquemonitoring technology in deep excavation," *Science Technology and Engineering*, vol. 8, no. 23, pp. 6406–6409, 2008.

[30] G.-H. Wang, Y.-C. Zhao, and Z.-F. Wang, "Influence of deep foundation pit construction insoft ground to adjacent buildings," *Construction Technology*, vol. 37, no. 9, pp. 16–18, 2008.

[31] A.-L. Ran, M.-G. Li, and J.-J. Chen, "Deformation behaviors of joint between shield tunnel and underground station impacted by connected deep foundation Pit," *Tunnel Construction*, vol. 36, no. 7, pp. 844–850, 2016, (in Chinese).

[32] X. Wang, "Comparison and analysis of several commonly used foundation pit deformation prediction models," *Journal of Shanxi Da tong University (Natural Science Edition)*, vol. 1, pp. 62–65, 2016, (in Chinese).

[33] C. Q. Dai and L. Wang, "VAR modeling of construction deformation prediction of deep foundation pit and application," *Rock and Soil Mechanics*, vol. 33, no. Sup 2, pp. 395–400, 2012, (in Chinese).

[34] W. G. Zhao, L. Y. Wang, and Z. X. Zhang, "Supply-demand-based optimization: a novel economics- inspired algorithm for global optimization," *IEEE Access*, vol. 7, pp. 73182–73206, 2019.

[35] Y. Li, W. Wang, and J. Wang, *Intelligent Optimization of Water Resources and Environment Model [M]*, Science Press, Beijing, 2014, (in Chinese).